HEPATOLOGY

HEPATOLOGY, VOL. 63, NO. 3, 2016

Macrophage Recruitment by Fibrocystin-Defective Biliary Epithelial Cells Promotes Portal Fibrosis in Congenital Hepatic Fibrosis

Luigi Locatelli,[1*] Massimiliano Cadamuro,[1,2*] Carlo Spirlì,[3] Romina Fiorotto,[3] Silvia Lecchi,[4] Carola Maria Morell,[1] Yury Popov,[5] Roberto Scirpo,[1] Maria De Matteis,[2] Mariangela Amenduni,[3] Andrea Pietrobattista,[6] Giuliano Torre,[6] Detlef Schuppan,[5,7] Luca Fabris,[2,3] and Mario Strazzabosco[1,3]

Congenital hepatic fibrosis (CHF) is a disease of the biliary epithelium characterized by bile duct changes resembling ductal plate malformations and by progressive peribiliary fibrosis, in the absence of overt necroinflammation. Progressive liver fibrosis leads to portal hypertension and liver failure; however, the mechanisms leading to fibrosis in CHF remain elusive. CHF is caused by mutations in *PKHD1*, a gene encoding for fibrocystin, a ciliary protein expressed in cholangiocytes. Using a fibrocystin-defective (*Pkhd1*$^{del4/del4}$) mouse, which is orthologous of CHF, we show that *Pkhd1*$^{del4/del4}$ cholangiocytes are characterized by a β-catenin-dependent secretion of a range of chemokines, including chemokine (C-X-C motif) ligands 1, 10, and 12, which stimulate bone marrow-derived macrophage recruitment. We also show that *Pkhd1*$^{del4/del4}$ cholangiocytes, in turn, respond to proinflammatory cytokines released by macrophages by up-regulating αvβ6 integrin, an activator of latent local transforming growth factor-β1. While the macrophage infiltrate is initially dominated by the M1 phenotype, the profibrogenic M2 phenotype increases with disease progression, along with the number of portal myofibroblasts. Consistent with these findings, clodronate-induced macrophage depletion results in a significant reduction of portal fibrosis and portal hypertension as well as of liver cysts. *Conclusion:* Fibrosis can be initiated by an epithelial cell dysfunction, leading to low-grade inflammation, macrophage recruitment, and collagen deposition; these findings establish a new paradigm for biliary fibrosis and represent a model to understand the relationship between cell dysfunction, parainflammation, liver fibrosis, and macrophage polarization over time. (HEPATOLOGY 2016;63:965-982)

Untreated chronic liver diseases lead to cirrhosis, portal hypertension, and clinical decompensation. The main mechanism of disease progression is liver fibrosis, i.e., the deposition of collagen in the portal space and/or around the hepatocytes, which is responsible for architectural distortion and vascular changes. Liver fibrosis is usually the result of an ongoing reparative response to unresolving necroinflammatory damage to the liver epithelia. However, some liver conditions, such as hepatoportal sclerosis and congenital hepatic fibrosis, do not follow this paradigm; and fibrosis appears to be rather caused by a nonclassical inflammatory process in the portal space without necrotic damage.

Abbreviations: CHF, congenital hepatic fibrosis; COL1(A1), procollagen α1(I); CXCL, chemokine (C-X-C motif) ligand; ELN, elastin; FPC, fibrocystin/polyductin; IL, interleukin; iNOS, inducible nitric oxide synthase; K19, cytokeratin-19; LCM, laser capture microdissection; MCP-1, monocyte chemotactic protein-1; mRNA, messenger RNA; α-SMA, α-smooth muscle actin; TGFβ, transforming growth factor-β; TGFβRI/TGFβRII, TGFβ receptors I and II; TNFα, tumor necrosis factor-α; WT, wild type.

Received July 9, 2015; accepted December 2, 2015.

Additional Supporting Information may be found at onlinelibrary.wiley.com/doi/10.1002/hep.28382/suppinfo.

**These authors contributed equally to this work.*

Supported by Telethon (GGP09189) and Progetto di Ricerca Ateneo 2011 (CPD113799/11) (to L.F., L.L., and M.C.); by National Institutes of Health grants DK079005 and DK034989 and the Silvio O. Conte Digestive Diseases Research Core Centers (projects CARIPLO 2011-0470 and PRIN 2009ARYX4T_005, to M.S.); by a PSC Partners Seeking a Cure grant (to M.S. and R.F.); and by National Institutes of Health grants 1R21A1 DK076873 and U19 AI066313 (to D.S.) and RO1DK101528 (to C.S.).

Congenital hepatic fibrosis (CHF) is a genetic cholangiopathy caused by mutations in *PKHD1*, the gene encoding for fibrocystin/polyductin (FPC), a protein of unknown function expressed on cilia and centromers of bile duct and renal tubular epithelial cells.[1,2] In the liver, FPC deficiency leads to the formation of biliary microhamartomas and segmental dilations of bile ducts accompanied by progressive portal fibrosis, resulting in clinically relevant portal hypertension.[3] Complications of portal hypertension are a major cause of morbidity and mortality in CHF.[4] It is expected that the ability to reduce the progression of fibrosis in CHF would improve survival. Unfortunately, the mechanisms responsible for portal fibrosis in CHF are unknown.

Recent studies have identified several defects of intracellular signaling in FPC-deficient cells, including increased cyclic adenosine monophosphate/protein kinase A signaling[5] and protein kinase A-dependent β-catenin activation.[5] β-Catenin is emerging as a novel regulator of inflammation, able to influence cytokine secretion in experimental liver cancer.[6] It has been proposed that a persistent, nonresolving cell dysfunction may promote a chronic, low-grade inflammatory response (defined by Medzhitov as "parainflammation") that can ultimately lead to scarring.[7] Interestingly, increased production of proinflammatory cytokines has been reported in fibropolycystic liver diseases.[8,9]

In this study, we used a mouse orthologous of human CHF that harbors a homozygous deletion in exon4 of the *Pkhd1* gene[10] to investigate the pathogenesis of liver fibrosis in CHF. Our data provide strong evidence that fibrosis is the result of a low-level chronic inflammatory response generated by FPC-defective cholangiocytes that secrete chemokines able to recruit bone marrow-derived macrophages and, in turn, respond to cytokines released by macrophages by up-regulating the $\alpha v\beta 6$ integrin, a local transforming growth factor-$\beta 1$ (TGF$\beta 1$) activator. In contrast with other experimental models of liver fibrosis, collagen deposition in *Pkhd1*$^{del4/del4}$ mice initiates with little contribution from myofibroblasts but then accelerates as the proportion of M2 polarized macrophages, TGF$\beta 1$ production, and portal myofibroblasts increase. In line with these data, macrophage depletion with clodronate reduces $\alpha v\beta 6$ integrin biliary expression and myofibroblast accumulation and halts fibrosis progression and the development of portal hypertension, in conjunction with a significant reduction in liver cysts. Our results provide a new paradigm for biliary fibrosis and represent a model to understand the relationship between cell dysfunction, parainflammation, liver fibrosis, and macrophage polarization over time.

Materials and Methods

ANIMAL MODEL

We used the Pkhd1$^{del4/del4}$ mouse (a kind gift from S. Somlo, Yale University, New Haven, CT), an

View this article online at wileyonlinelibrary.com.
DOI 10.1002/hep.28382

Potential conflict of interest: Dr. Schuppan consults and received grants from Boehringer-Ingelheim. He consults for Novartis, Takeda, Mitsubishi, Nimbus, Johnson & Johnson, Alnylam, Pronova, and Roivant.

ARTICLE INFORMATION:

From the [1]Department of Surgery and Translational Medicine, University of Milan-Bicocca, Milan, Italy; [2]Department of Molecular Medicine, University of Padua School of Medicine, Padua, Italy; [3]Section of Digestive Diseases, Yale University, New Haven, CT; [4]Center for Liver Research (CeLiveR), Papa Giovanni XXIII Hospital, Bergamo, Italy; [5]Division of Gastroenterology, Beth Israel Deaconess Medical Center, Harvard Medical School, Boston, MA; [6]Liver Unit, Bambino Gesù Pediatric Hospital, IRCSS, Rome, Italy; [7]Institute of Translational Immunology, Johannes Gutenberg University, Mainz, Germany.

ADDRESS CORRESPONDENCE AND REPRINT REQUESTS TO:

Luca Fabris M.D., Ph.D.
Department of Molecular Medicine
University of Padua School of Medicine
Viale G. Colombo 3, 35131 Padua, Italy.
E-mail: luca.fabris@unipd.it
luca.fabris@yale.edu
Tel: +39 049 827 6127
Fax: +39 049 807 3310.

accepted model for human CHF disease.[10] All animals were housed at the Yale Animal Care facility and received humane care according to the Yale Institutional Animal Care and Use Committee protocols. See Supporting Information for mouse model details.

ASSESSMENT OF PORTAL FIBROSIS BY SIRIUS RED STAINING

Sirius red histochemistry was performed to assess the extension of portal fibrosis and its progression through maturation. Liver sections were obtained from *Pkhd1*$^{del4/del4}$ and wild-type (WT) mice at different maturation ages. See Supporting Information for details.

ASSESSMENT OF PORTAL HYPERTENSION

Portal hypertension was assessed by measuring the spleen weight in the same mice analyzed for portal fibrosis. For each animal, the spleen weight was normalized to the respective body weight and used as a measure of portal hypertension.[11]

IN VIVO CLODRONATE TREATMENT

To induce a selective macrophage depletion, *Pkhd1*$^{del4/del4}$ mice of 3 months of age were treated for 3 months with clodronate liposomes (100 mg/kg every 3 days intraperitoneally, n = 4) or with vehicle (sterile phosphate-buffered saline + liposomes every 3 days intraperitoneally, n = 3).[12] At the end of treatment, mice were sacrificed to assess the extent of peribiliary fibrosis by sirius red; the cystic area by immunohistochemistry for cytokeratin-19 (K19); the number of α-smooth muscle actin-positive (α-SMA$^+$), F4/80$^+$, and CD45$^+$ cells in the portal area; the number of αvβ6 integrin$^+$ cysts; and the spleen/body weight ratio.

HUMAN TISSUES SAMPLES OF CHF

Formalin-fixed, paraffin-embedded archival tissue specimens of CHF patients obtained from percutaneous needle liver biopsy (n = 3) and surgical specimens from liver transplant explants (n = 2) or liver resection (n = 1) were considered for the immunohistochemical study. All specimens were reviewed to confirm the histopathological diagnosis of CHF. Patients undergoing liver transplantation or liver resection were complicated by portal hypertension, which instead was absent in patients undergoing needle biopsy. Informed consent and local regional ethical committee approval were obtained before tissue collection.

EXPRESSION OF αVβ6 INTEGRIN, SNAIL1, P-SMAD3, AND PHENOTYPIC CHARACTERIZATION OF THE PORTAL INFLAMMATORY CELL INFILTRATE BY IMMUNOHISTOCHEMISTRY IN HUMAN AND MURINE SAMPLES

Liver tissue sections obtained from both *Pkhd1*$^{del4/del4}$ mice and archived biopsies of CHF patients with different degrees of portal fibrosis were considered to study the expression of αvβ6 integrin along with Snail1 and pSmad3 as signatures of TGFβ1 activation and the phenotype of the portal cell infiltrate using the following markers: K19 (cholangiocyte), CD45 (leukocyte), NIMP-R14 (neutrophil), F4/80 (macrophage), MAC387 (bone marrow-derived macrophage), CD68 (resident macrophage), inducible nitric oxide synthase (iNOS; M1 macrophage), CD206 (M2 macrophage), collagen-I, α-SMA (myofibroblast), and elastin (ELN, portal myofibroblast). See Supporting Information for details.

Quantification of K19$^+$, α-SMA$^+$, ELN$^+$, CD45$^+$, F4/80$^+$/iNOS$^+$, and F4/80$^+$/CD206$^+$ cells as well as αvβ6 integrin expression by immunohistochemistry are described in the Supporting Information.

EXPRESSION OF β6 MESSENGER RNA, FIBROSIS-RELATED TRANSCRIPTS, AND CYTOKINES/CHEMOKINES BY QUANTITATIVE REAL-TIME REVERSE-TRANSCRIPTION POLYMERASE CHAIN REACTION

Total RNA was isolated from liver tissue as described,[13] to measure the expression of β6 integrin, TGFβ1, tumor necrosis factor-α (TNFα), and procollagen α1(I) (COL1[A1]), as reported.[14] See the Supporting Information for further details.

LIVER NONPARENCHYMAL CELL ISOLATION AND FLUORESCENCE-ACTIVATED CELL SORTING ANALYSIS

Fluorescence-activated cell sorting analysis was performed to characterize the different cell subsets contributing to the portal inflammatory cell infiltrate. Liver nonparenchymal cells were isolated in the Cell Isolation Core of the Yale Liver Center. See the Supporting Information for details.

ISOLATION AND CHARACTERIZATION OF CHOLANGIOCYTES

Mouse cholangiocytes were isolated from *Pkhd1*$^{del4/del4}$ and WT mice at 3 months of age as described.[5]

MACROPHAGE RECRUITMENT BY CONDITIONED MEDIA FROM *PKHD1*$^{DEL4/DEL4}$ CHOLANGIOCYTES

To test the polarity-dependent ability of *Pkhd1*$^{del4/del4}$ cholangiocytes to recruit macrophages, we studied the effect of conditioned medium differentially harvested from basolateral and apical sides on a mouse macrophage cell line (RAW264.7). Further information is detailed in the Supporting Information.

ASSESSMENT OF MACROPHAGE MIGRATION INDUCED BY CHEMOKINE (C-X-C MOTIF) LIGANDS 1 AND 10

To evaluate whether cytokines significantly secreted by *Pkhd1*$^{del4/del4}$ cholangiocytes in the basolateral medium (chemokine [C-X-C motif] ligand 1 [CXCL1], CXCL10) could represent homing signals for inflammatory cells, we studied their ability to stimulate cell migration in macrophages, using murine RAW 264.7 macrophages. The mouse recombinant proteins CXCL1 and CXCL10 (PeproTech, London, UK) were tested at a dose of 1 ng/mL in Boyden chambers.

DETERMINATION OF CYTOKINE SECRETION IN *PKHD1*$^{DEL4/DEL4}$ CHOLANGIOCYTES

In supernatant from the basolateral and apical sides of the polarized cholangiocyte monolayer, a panel of 32 mouse chemokines and cytokines (see Supporting Table S1) was analyzed using the Millipore MILLIPLEX mouse cytokines/chemokines kit coupled with the BioPlex Luminex platform. See Supporting Information for details.

ASSESSMENT OF MACROPHAGE PRODUCTION OF TGFβ1 AND TNFα INDUCED BY CXCL1 AND CXCL10

To evaluate whether CXCL1, CXCL10, and CXCL12 were also able to induce cytokine secretion by inflammatory cells, we studied their ability to stimulate expression of TGFβ1 and TNFα transcripts in RAW 264.7 cells. Cultured macrophages were tested with the mouse recombinant proteins CXCL1 and CXCL10 (PeproTech) at 1 ng/mL and CXCL12 (R&D Systems, Milan, Italy) at 100 μg/mL for 12 hours. Further details are given in the Supporting Information.

EFFECTS OF TGFβ1 AND TNFα ON β6 MESSENGER RNA EXPRESSION ON CULTURED CHOLANGIOCYTES BEFORE AND AFTER INHIBITION OF TGFβ RECEPTOR II

To ascertain if TNFα stimulated separate signaling pathways to directly modulate β6 expression, independently from a TGFβ1 loop, experiments on cytokine stimulation were run before and after preincubation for 24 hours of cultured cholangiocytes with a dominant negative, recombinant soluble TGFβ receptor type II (TGFβRII)-Fc fusion protein (10 ng/mL; kind gift of Stromedix/Biogen, Inc.). Recombinant soluble TGFβRII-FC fusion protein is a chimeric construct inhibiting TGFβ1 signaling, in which the extracellular portion of TGFβRII was fused to an immunoglobulin heavy chain Fc fragment. By blocking specifically TGFβRII, this antibody prevents the association of TGFβRII with TGFβRI and, therefore, its

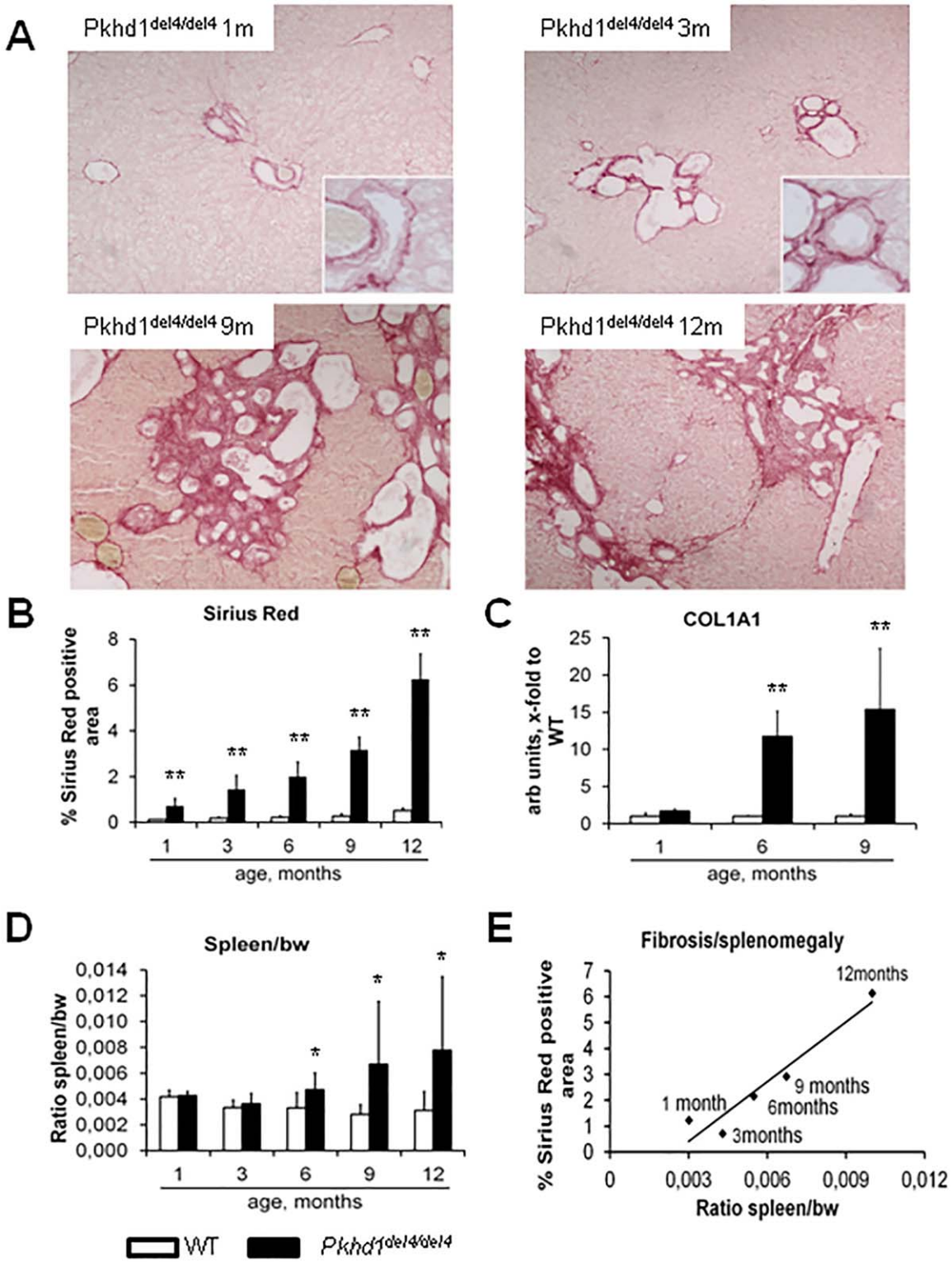

FIG. 1. Age-dependent increase in peribiliary fibrosis correlates with portal hypertension in *Pkhd1*$^{del4/del4}$ mice. (A) Micrographs of sirius red-stained liver sections taken from WT and *Pkhd1*$^{del4/del4}$ mice of different ages and indicating that peribiliary fibrosis develops progressively, starting at the pericystic region and then extending through the portal area, finally leading to portoportal septa formation (sirius red, magnification ×100). (B) Morphometric analysis of sirius red-stained *Pkhd1*$^{del4/del4}$ mouse livers trough maturation (percent covered by sirius red, n = 4-7 for each age). (C) Similarly, gene expression of COL1(A1) in whole-liver lysates increased slowly, reaching a 15-fold increase at 9 months (n = 3 for each age). (D) Splenomegaly (measured as the spleen weight/body weight), a surrogate marker of portal hypertension in CHF, became significant at 6 months and increased thereafter (n = 4-7 for each age). (E) The extent of portal fibrosis (sirius red) strongly and positively correlated with splenomegaly ($r = 0.96$, $P < 0.01$). *$P < 0.05$ versus WT (same age), **$P <$ 0.01 versus WT (same age). Abbreviation: bw, body weight.

phosphorylation. See Supporting Information for details.

EFFECTS OF TGFβ1 ON COL1(A1) AND SNAIL1 MESSENGER RNA EXPRESSION BY CULTURED CHOLANGIOCYTES

After starvation for 24 hours, polarized cultured primary cholangiocytes were treated for 24 hours with the recombinant murine TGFβ1 (1 ng/mL). Before and after TGFβ1 stimulation, COL1(A1), and Snail1 messenger RNA (mRNA) expression was determined in total RNA from cultured cells (see above).

Statistical analysis is detailed in the Supporting Information.

Results

PKHD1$^{DEL4/DEL4}$ MICE AS A DISEASE MODEL FOR CHF

Pkhd1$^{del4/del4}$ mice bear an inactivating deletion in the exon 4 of the *Pkhd1* gene.[10] Serial analysis of *Pkhd1*$^{del4/del4}$ mouse liver and spleen demonstrated an age-dependent increase in the biliary cystic malformations (Supporting Fig. S1A,B); peribiliary fibrosis (Fig. 1A); increased collagen-I deposition, as shown by the progressive increase in sirius red staining (Fig. 1B); and increased COL1(A1) gene expression compared to WT littermates (Fig. 1C). Deposition of fibrosis began in the pericystic region and then extended through the portal area, finally leading to portoportal septa formation (Fig. 1A). Significant splenomegaly, indicative of clinical portal hypertension, became evident between 6 and 9 months after birth and increased further up to 12 months of age (Fig. 1D); splenomegaly strongly correlated with sirius red staining ($r = 0.96$, $P < 0.01$) (Fig. 1E). The histological biliary lesions and the slow progression of fibrosis, leading to portal hypertension, are consistent with the morphology and the natural history of human CHF and establish *Pkhd1*$^{del4/del4}$ mice as a reliable disease model.

EARLY PERIBILIARY INFILTRATION WITH CD45$^+$ CELLS, MOSTLY MACROPHAGES

Development of pericystic fibrosis was associated with the progressive accumulation of inflammatory cells in the portal tracts, which localized in close vicinity to the biliary cysts, as observed by immunohistochemistry for CD45$^+$ (Fig. 2A). By 9 months of age the percentage of the portal tract area infiltrated by CD45$^+$ cells increased to 25% (Fig. 2B). In contrast, the number of myofibroblasts (α-SMA$^+$ cells) was initially limited (Fig. 2C,D); these cells were positive for the portal fibroblast biomarker ELN, and their number similarly increased progressively (Fig. 2E,F). Phenotypic characterization of the inflammatory cell infiltrate by fluorescence-activated cell sorting analysis (CD45$^+$-based cell selection) and by combined immunohistology for CD45 and F4/80 (macrophage marker) or NIMP-R14 (neutrophil marker) showed that the majority of the infiltrating CD45$^+$ cells were macrophages, based on their coexpression of CD11b and F4/80 (Supporting Fig. S2A). The percentage of CD45$^+$/CD11b$^+$/F4/80$^+$ cells ranged from 57% to 68% of the total CD45$^+$ cell population without significant changes over time. The contribution of neutrophils (CD45$^+$/Ly6G$^+$) and monocytes (CD45$^+$/CD11b$^+$/Ly6G$^-$/F4/80$^-$) was consistently much lower than that of macrophages (Supporting Fig. S2B). Immunohistochemistry showed that the majority of CD45$^+$ cells were F4/80$^+$ and were localized in the portal space along the profile of the cysts (Supporting Fig. S2C,E). In contrast with F4/80 cells, NIMP-R14$^+$ cells contributed minimally to the CD45$^+$ cell population, being limited to small cell clumps (Supporting Fig. S2D). By dual immunofluorescence for CD68 (marker of local resident macrophages) and MAC387 (marker of bone marrow-derived macrophages) combined with the biliary marker K19, we found that peribiliary macrophages predominantly expressed MAC387, while the number of CD68$^+$ cells infiltrating the portal area was negligible until 9 months (Supporting Fig. S3A,B). Microbiological analysis showed that *Pkhd1*$^{del4/del4}$ livers from all ages were sterile (not shown); in addition, gut decontamination with polymyxin B and neomycin had no effect on the progressive accumulation of CD45$^+$ cells in the portal space (not shown). The preponderance of CD45$^+$ inflammatory cells on α-SMA$^+$ myofibroblasts and ELN$^+$ portal fibroblasts in the peribiliary infiltrate was confirmed in liver biopsies from CHF patients at a stage not yet complicated by portal hypertension (Supporting Fig. S4A); α-SMA$^+$ myofibroblasts and ELN$^+$ portal myofibroblasts became prevalent in more advanced cases undergoing liver transplantation because of complications of portal hypertension (Supporting Fig. S4B).

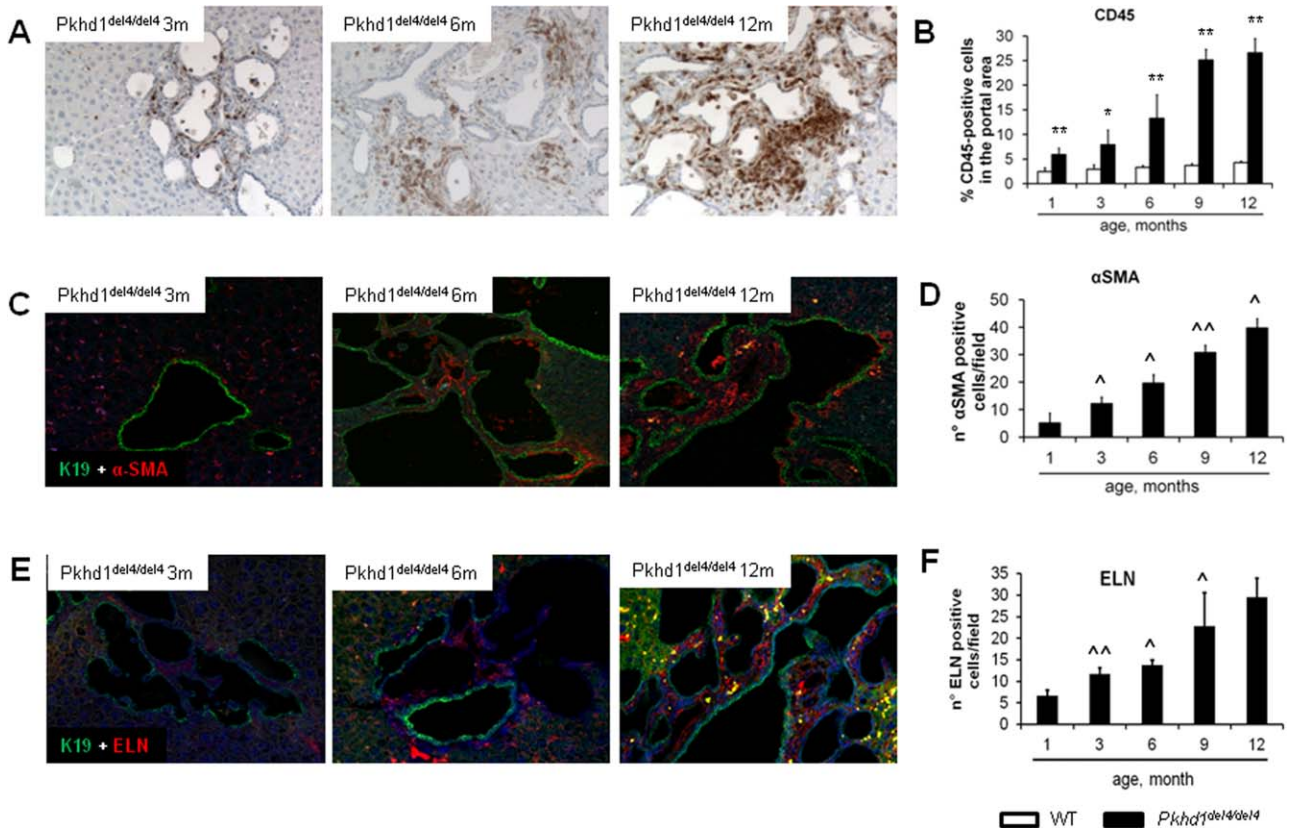

FIG. 2. Progressive peribiliary accumulation of inflammatory cells in the portal tract, coexpressing F4/80 (macrophage marker) contrasts with the initial scarce contribution of myofibroblasts. (A) A progressive portal accumulation of $CD45^+$ inflammatory cells adjacent to biliary cysts was observed (immunoperoxidase for CD45, magnification ×200). (B) $CD45^+$ cells were quantified by morphometric analysis (n = 3 for each age). (C) In *Pkhd1*$^{del4/del4}$ mice, α-SMA^+ myofibroblasts scattered within the portal space (dual immunofluorescence for α-SMA, in red, and K19, in green; magnification ×200). (D) The number increased slowly through maturation with a linear pattern (n = 3 for each age). (E) Similarly to α-SMA, ELN^+ portal fibroblasts accumulated in the portal space in a time-dependent fashion (dual immunofluorescence for ELN, in red, and K19, in green; magnification ×200). (F) As quantified by morphometry, the number of ELN^+ cells augmented through maturation, with the most relevant increase after 6 months (n = 4 for each age). $^*P < 0.05$ versus WT (same age), $^{**}P < 0.01$ versus WT (same age), $^{\wedge}P < 0.05$ versus previous maturation age, $^{\wedge\wedge}P < 0.01$ versus previous maturation age.

CHANGES IN MACROPHAGE POLARIZATION OVER TIME

Among $F4/80^+$ cells, the subset coexpressing iNOS (M1 polarization marker) was preponderant over that coexpressing CD206 (M2 marker). However, the relative contribution of M2 macrophages increased progressively, matching that of M1 at 12 months (Fig. 3A-C). Consistent with this observation, hepatic gene expression of TGFβ1 (an M2 cytokine) was only modestly increased in the early phases, becoming significant at 9 months (2.5-fold with respect to WT) (Fig. 3D), whereas TNFα (an M1 cytokine) mRNA was strongly up-regulated from the early stage of the disease, reaching 80-fold expression with respect to WT at 9 months (Fig. 3E).

EXPRESSION OF αVβ6 INTEGRIN, AN ACTIVATOR OF LATENT TGFβ1, IS UP-REGULATED IN THE CYSTIC EPITHELIUM OF *PKHD1*$^{DEL4/DEL4}$ MICE IN RESPONSE TO THE MACROPHAGE-DERIVED CYTOKINES TGFβ1 AND TNFα

The αvβ6 integrin, an activator of latent TGFβ1 that is expressed by reactive cholangiocytes during liver repair, increased progressively between 1 and 12 months (Fig. 4A,B). Expression of αvβ6 integrin was restricted to biliary cysts and was negative in bile ducts

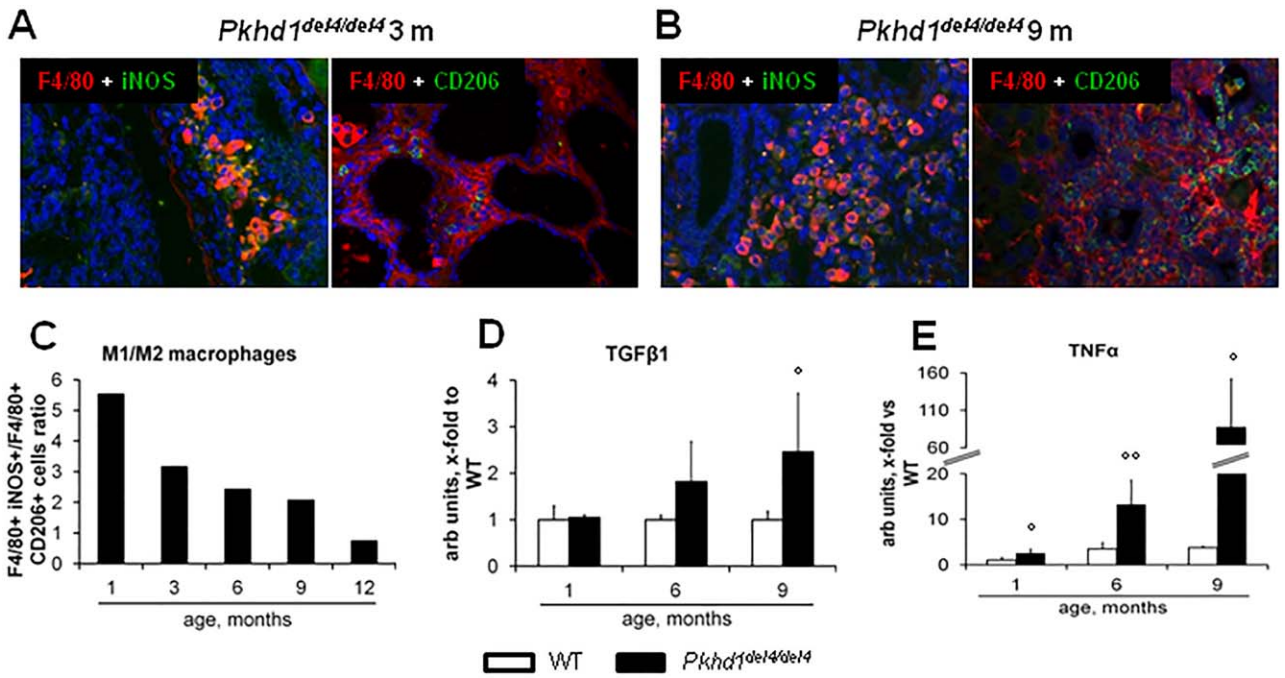

FIG. 3. The initial M1 macrophage infiltrate is matched by M2 cells. (A,B) By dual immunofluorescence with the macrophage marker F4/80 (red), we evaluated the relative proportion of the macrophage phenotypes in the portal infiltrate, M1 (iNOS$^+$, green) and M2 (CD206$^+$, green), through the different ages (A, representative sample, 3 months; B, representative sample, 9 months, magnification ×200). (C) Until the ninth month, the macrophage population was dominated by the M1 phenotype; but the relative proportion of M2 macrophages increased progressively, reaching that of M1 at the twelfth month, as shown by the changes in the M1/M2 ratio through maturation (n = 3 for each age). (D) Consistent with this temporal sequence, gene expression of TGFβ1 (an M2 cytokine) in the whole liver increased mildly in the first phase, becoming significant only at 9 months (2.5-fold with respect to WT) (n = 3 for each age). (E) Up-regulation of TNFα (an M1 cytokine) was instead evident from the early stage of the disease, reaching 80-fold expression with respect to WT livers at 9 months (n = 3 for each age). $^\circ P < 0.05$ versus WT (1 month), $^{\circ\circ}P < 0.01$ versus WT (1 month).

of WT littermates. The immunohistochemical expression of $\alpha v\beta 6$ integrin on cystic epithelia strongly correlated with portal fibrosis as measured by sirius red ($r = 0.94$, $P < 0.02$) (Fig. 4C). Notably, $\alpha v\beta 6$ integrin was expressed in cysts surrounded by a dense macrophage infiltrate (Fig. 4E), and the number of $\alpha v\beta 6$ integrin$^+$ cysts correlated with the extent of CD45$^+$ cell infiltration ($r = 0.97$, $P < 0.01$) (Fig. 4D), thereby suggesting a relationship between peribiliary recruitment of inflammatory cells and $\alpha v\beta 6$ up-regulation in biliary cysts.

Thus, we studied whether the macrophage-derived cytokines TNFα and TGFβ1 were able to regulate the expression of $\beta 6$ (the rate-limiting subunit for the formation of the $\alpha v\beta 6$ integrin dimer) mRNA in cultured *Pkhd1*$^{del4/del4}$ cholangiocytes. We found that $\beta 6$ mRNA, already significantly increased in basal conditions in *Pkhd1*$^{del4/del4}$ cholangiocytes compared with WT, was further and significantly increased by stimulation with either TNFα or TGFβ1 ($P < 0.05$). Blockade of the TGFβRII receptor abolished the effects of TGFβ1 on $\beta 6$ gene expression but not those of TNFα (Fig. 4F), indicating that TNFα effects are TGFβ1-independent. Interestingly, the stimulatory effect of TNFα on $\beta 6$ was observed only in *Pkhd1*$^{del4/del4}$ cholangiocytes that already have increased expression levels of $\beta 6$, an observation again consistent with a proinflammatory phenotype of cystic cells in FPC deficiency. The ability of TNFα to up-regulate $\alpha v\beta 6$, thereby activating latent TGFβ1, is likely involved in peribiliary collagen deposition in the early phases of the disease, when TGFβ1 expression is only mildly up-regulated and M1 macrophages predominate.

Immunohistochemical analysis of serial liver sections from *Pkhd1*$^{del4/del4}$ mice and from archival

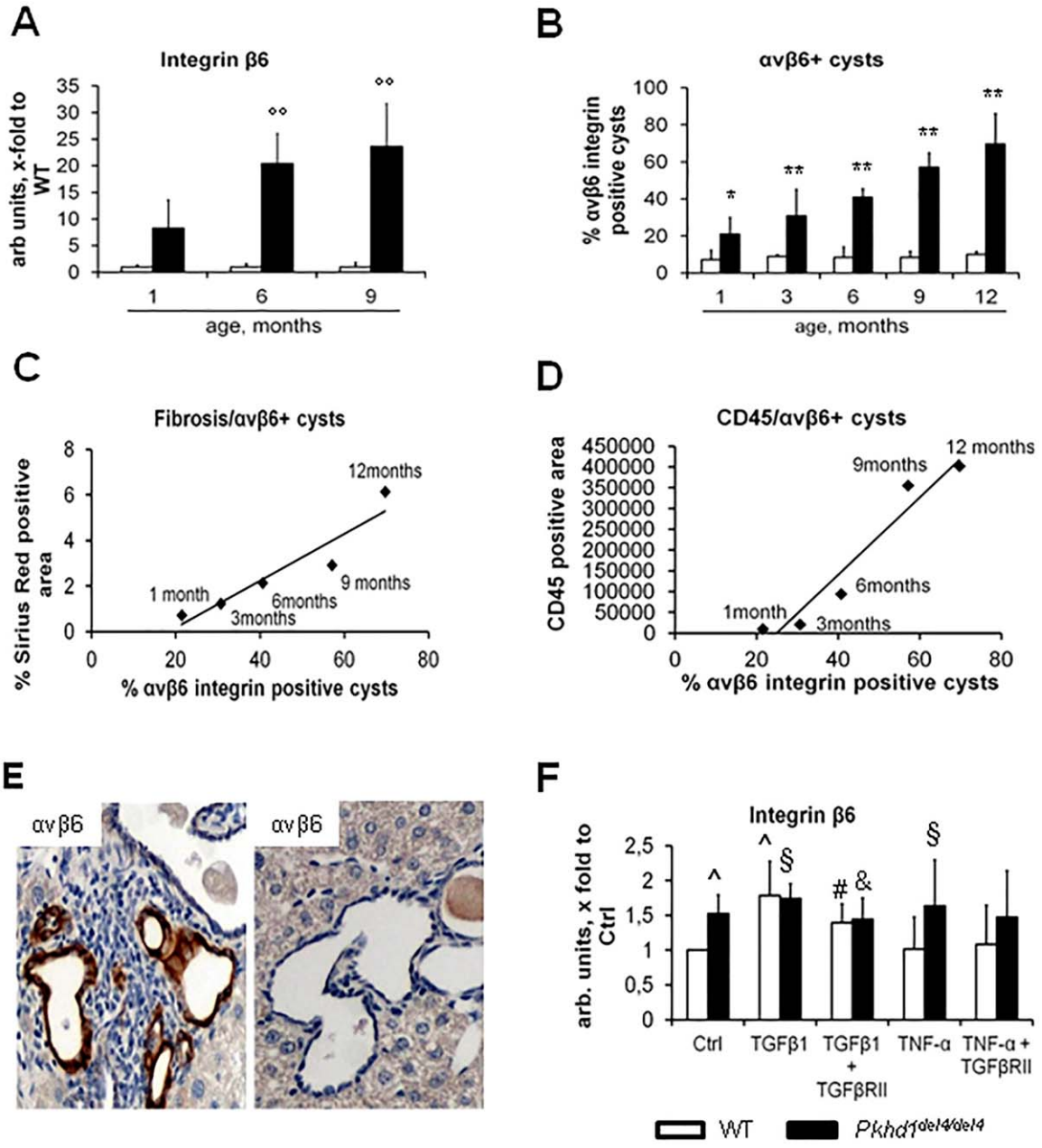

FIG. 4. αvβ6 integrin expression correlates with portal fibrosis and peribiliary accumulation of $CD45^{+}$ cells in $Pkhd1^{del4/del4}$ mice. (A) In contrast with WT mice, $Pkhd1^{del4/del4}$ mice showed a progressive increase in β6 gene expression in whole liver, which was greater than 25-fold at 6 months and nearly 35-fold at 9 months (n = 3 for each age). (B) Similarly, αvβ6 integrin expression on cyst epithelia assessed by immunohistochemistry increased progressively, reaching nearly 70% of biliary structures at 12 months (n = 3-5 for each age). (C,D) Immunohistochemical expression of αvβ6 strongly correlated both with portal fibrosis ($r = 0.94$, $P < 0.02$) and with the $CD45^{+}$ portal cell infiltrate ($r = 0.97$, $P < 0.01$). (E) In any given specimen, αvβ6 integrin was typically higher in biliary cysts surrounded by a dense inflammatory infiltrate (immunoperoxidase for αvβ6, representative sample, 6 months, magnification ×400). (F) TGFβ1 and TNFα stimulate gene expression of β6 integrin in $Pkhd1^{del4/del4}$ cholangiocytes. In $Pkhd1^{del4/del4}$ cholangiocytes, β6 mRNA was significantly increased in basal conditions with respect to WT. In both WT and $Pkhd1^{del4/del4}$ cholangiocytes, β6 expression was further and significantly increased after TGFβ1. Unlike TGFβ1, TNFα significantly increased β6 mRNA expression only in $Pkhd1^{del4/del4}$ cholangiocytes. TGFβRII blockade abolished the TGFβ1 effects on β6 mRNA expression in both $Pkhd1^{del4/del4}$ and WT cholangiocytes, in contrast to TNFα whose effects on β6 were unaffected by TGFβRII antagonism (n = 6-10 for each experimental condition, cultured cholangiocytes derived from mice 3 months of age). $^{\circ\circ}P < 0.01$ versus WT (1 month), $^{*}P < 0.05$ versus WT (same age), $^{**}P < 0.01$ versus WT (same age), $^{\wedge}P < 0.05$ versus WT control, $^{\S}P < 0.05$ versus $Pkhd1^{del4/del4}$ control, $^{\#}P < 0.05$ versus WT TGFβ1-treated, $^{\&}P < 0.05$ versus $Pkhd1^{del4/del4}$ TGFβ1-treated.

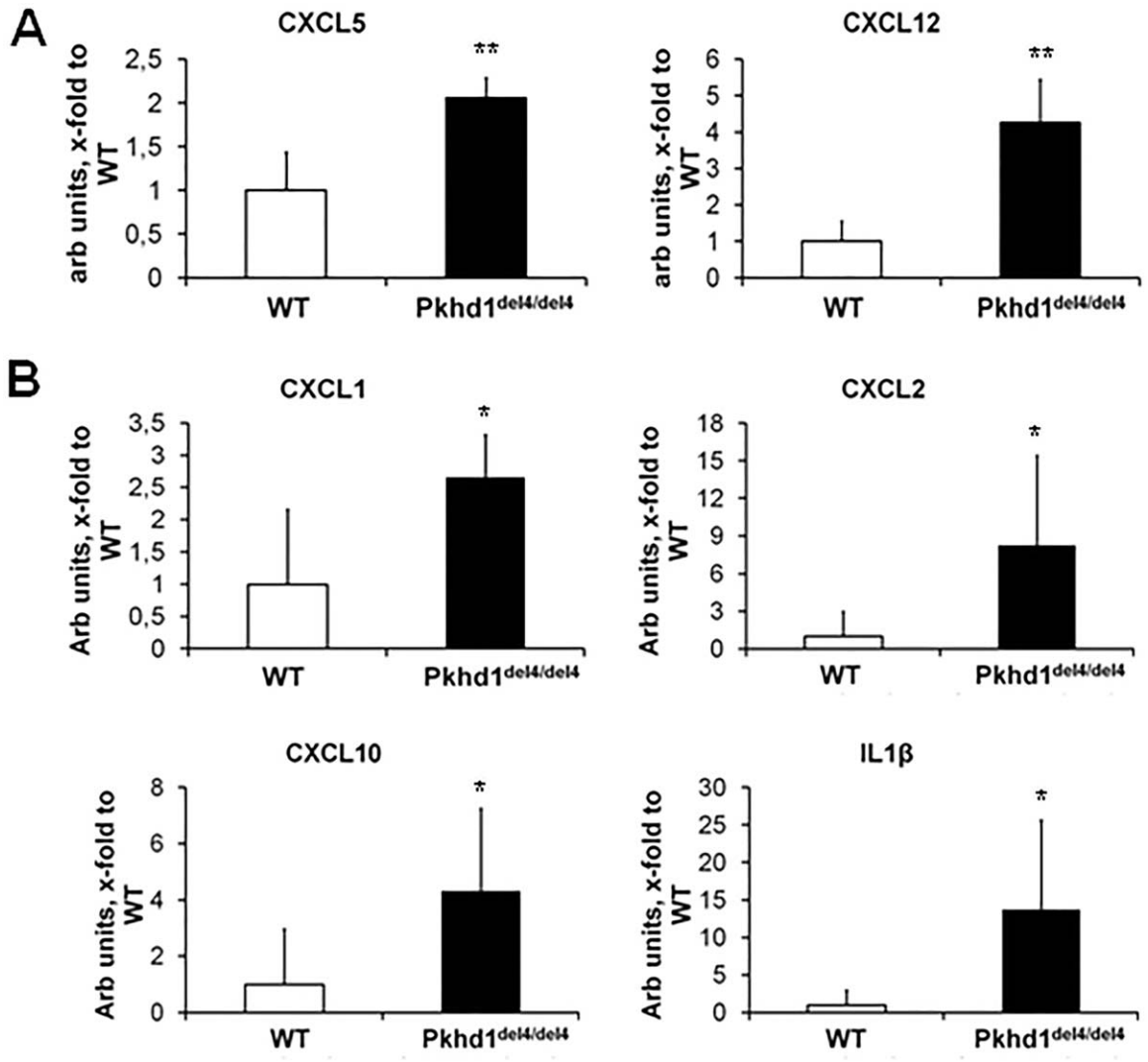

FIG. 5. Gene expression analysis of biliary K19-positive structures isolated from *Pkhd1*$^{del4/del4}$ and WT mice by LCM shows increases in CXCL5, CXCL12, CXCL1, CXCL2, CXCL10, and IL1β. To identify the soluble factors mediating macrophage recruitment by *Pkhd1*$^{del4/del4}$ cholangiocytes, gene expression of a number of cytokines previously shown to be secreted by cholangiocytes in culture was assessed in mRNA selectively captured from epithelial cells lining biliary cysts of *Pkhd1*$^{del4/del4}$ and normal ducts of WT mice at 1 month and 3 months of age by LCM. (A) LIX/CXCL5 and SDF1/CXCL12 were already significantly increased in biliary cysts of *Pkhd1*$^{del4/del4}$ mice at 1 month. (B) Also, keratinocyte chemoattractant/CXCL1, MIP-2/CXCL2, IP-10/CXCL10, SDF1/CXCL12, and IL-1β became significantly increased at 3 months of age (n = 4 for WT, n = 5 for *Pkhd1*$^{del4/del4}$ for both ages). $^{*}P < 0.05$ versus WT, $^{**}P < 0.01$ versus WT.

specimens of CHF patients showed nuclear expression of Snail1 and pSmad3 (transcription factors activated by TGFβ1 signaling) in cystic cells expressing $\alpha v\beta 6$ (Supporting Fig. S5). This finding provides clear evidence that TGFβ1 signaling is locally activated in $\alpha v\beta 6$-expressing cysts and that the findings described in *Pkhd1*$^{del4/del4}$ mice are actually relevant also for patients with CHF.

FACTORS SECRETED BY *PKHD1*$^{DEL4/DEL4}$ CHOLANGIOCYTES RECRUIT MACROPHAGES AT THEIR BASOLATERAL POLE

Having shown that in the early phases of the disease the pericystic spaces of *Pkhd1*$^{del4/del4}$ mice are infiltrated more by macrophages than by

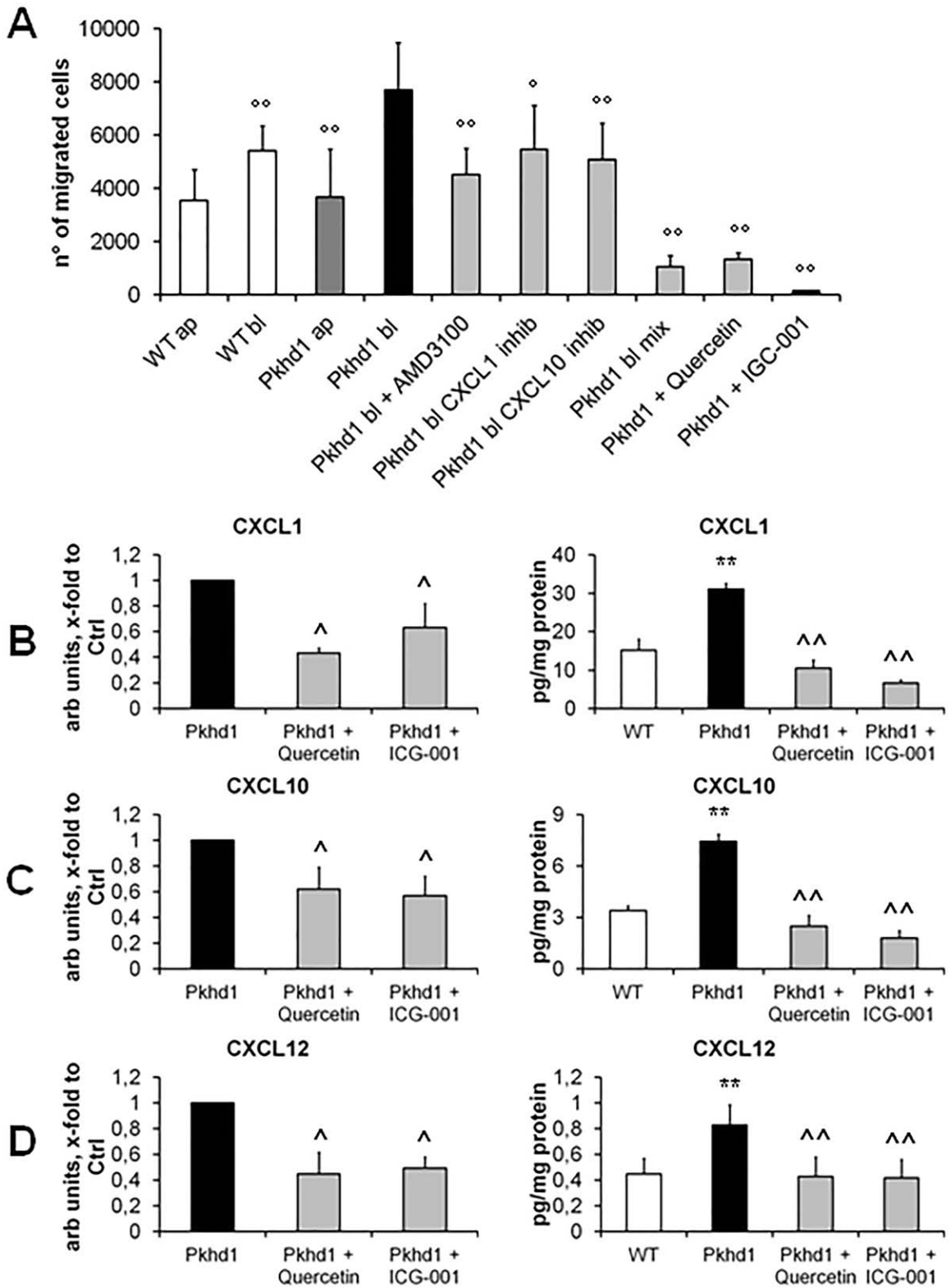
A
n° of migrated cells
10000
8000
6000
4000
2000
0
WT ap
WT bl
Pkhd1 ap
Pkhd1 bl
Pkhd1 bl + AMD3100
Pkhd1 bl CXCL1 inhib
Pkhd1 bl CXCL10 inhib
Pkhd1 bl mix
Pkhd1 + Quercetin
Pkhd1 + IGC-001
B
CXCL1
arb units, x-fold to Ctrl
pg/mg protein
Pkhd1
Pkhd1 + Quercetin
Pkhd1 + ICG-001
WT
C
CXCL10
D
CXCL12

FIG. 6.

myofibroblasts and that cytokines characteristic either of the M1 or the M2 polarization are able to up-regulate αvβ6 integrin, thereby promoting a pericystic fibrogenic response, we hypothesized that macrophages could be attracted into the pericystic area by soluble factors secreted by the *Pkhd1*$^{del4/del4}$ cholangiocytes themselves. Therefore, we studied the transwell migration of the macrophage cell line RAW 264.7, after exposure to conditioned medium collected from the apical or basolateral side of polarized monolayers of WT or *Pkhd1*$^{del4/del4}$ cholangiocytes (isolated from 3-month-old mice). Macrophage migration was significantly higher after exposure to conditioned medium from *Pkhd1*$^{del4/del4}$ than to that from WT cholangiocytes; furthermore, the basolateral medium from *Pkhd1*$^{del4/del4}$ cholangiocytes significantly stimulated macrophage recruitment and did so more strongly than the apical medium. Interestingly, recruitment of RAW 264.7 macrophages was significantly lower when challenged with conditioned medium from cells exposed to β-catenin inhibitors such as quercetin or ICG-001. Collectively, these data are consistent with the hypothesis that *Pkhd1*$^{del4/del4}$ cholangiocytes secrete paracrine factors that are able to recruit macrophages through a β-catenin-dependent mechanism.

To identify the factors possibly involved in macrophage recruitment by *Pkhd1*$^{del4/del4}$ cholangiocytes, we first measured the gene expression of a number of cytokines previously shown to be secreted by cholangiocytes in culture. We used laser capture microdissection (LCM) of the epithelial cysts in *Pkhd1*$^{del4/del4}$ versus bile ducts in WT littermates at 1 month and 3 months of age (Fig. 5). We found that increased gene expression of SDF-1/CXCL12 and LIX/CXCL5 represented the earliest changes in cystic structures of *Pkhd1*$^{del4/del4}$ mice (Fig. 5A), followed at 3 months by keratinocyte chemoattractant/CXCL1, IP-10/CXCL10, MIP-2/CXCL2 and interleukin-1β (IL-1β) (Fig. 5B). All these cytokines possess chemotactic functions for monocytes and macrophages. To verify that the above cytokines were actually secreted by *Pkhd1*$^{del4/del4}$ cholangiocytes, we measured their secretion at the basolateral medium of cultured cholangiocyte monolayers. Supporting Table S1 shows the cytokines/chemokines secreted into the basolateral medium by *Pkhd1*$^{del4/del4}$ cholangiocytes. Some of these, such as CXCL1, CXCL10, and CXCL12, were significantly more secreted by cultured *Pkhd1*$^{del4/del4}$ cells; others, including monocyte chemotactic protein-1 (MCP-1)/chemokine (C-C motif) ligand 2 and CXCL5, showed a clear trend toward increased secretion in *Pkhd1*$^{del4/del4}$ cholangiocytes with respect to WT.

CXCL12 is a well-known chemoattractant for macrophages[15]; less is known about CXCL1 and CXCL10. By exposing macrophages to the relative recombinant chemokines, we found that both CXCL1 and CXCL10 were able to significantly stimulate transwell migration of RAW 264.7 cells (Supporting Fig. S6A) (both 1 ng/mL). Furthermore, CXCL1 and CXCL10, but not CXCL12, were able to up-regulate the expression of TGFβ1 and TNFα transcript in macrophages (Supporting Fig. S6B,C). The pathogenetic relevance of the chemotactic effect of CXCL1, CXCL10, and CXCL12 on macrophages was confirmed by the significant reduction of macrophage migration after administration of their specific blocking antibodies or inhibitors to the basolateral conditioned medium of *Pkhd1*$^{del4/del4}$ cholangiocytes. Notably, the combined administration of the three specific blockers to the basolateral medium of the *Pkhd1*$^{del4/del4}$ cholangiocytes had a synergic effect of

FIG. 6. Basolateral conditioned medium of *Pkhd1*$^{del4/del4}$ cholangiocytes contains chemokines able to stimulate macrophage recruitment. (A) Migration of RAW 264.7 macrophages was measured in Boyden chambers containing conditioned medium. In *Pkhd1*$^{del4/del4}$ cholangiocytes, basolateral conditioned medium induced a stronger migratory effect of RAW 264.7 macrophages than apical medium or basolateral medium from WT cholangiocytes (n = 4 for both experiments). This effect was significantly inhibited by specific antagonism of CXCL1, CXCL10, and CXC12 and abolished by combined antagonism of CXCL1+CXCL10+CXCL12 or by inhibition of β-catenin signaling with quercetin (50 μM) or ICG-001 (25 μM) (n = 4 for each experiment). (B-D) Compared with WT, *Pkhd1*$^{del4/del4}$ cultured cholangiocytes expressed significantly higher amounts of CXCL1 (B), CXCL10 (C), and CXCL12 (D) both at the mRNA (n = 7 for each chemokine) and protein levels in the basolateral medium (n = 3 for CXCL1 and CXCL10, n = 12 for CXCL12); all chemokine expression levels were significantly reduced by inhibition of β-catenin signaling with quercetin (50 μM) or ICG-001 (25 μM) (n = 7 for each chemokine for reverse-transcription polymerase chain reaction experiments, n = 4 for each chemokine for enzyme-linked immunosorbent experiments) (cholangiocytes derived from mice 3 months of age). $^{**}P < 0.01$ versus WT, $^{\wedge}P < 0.05$ versus *Pkhd1*, $^{\wedge\wedge}P < 0.01$ versus *Pkhd1*, $^{\circ}P < 0.05$ versus *Pkhd1* basolateral medium, $^{\circ\circ}P < 0.01$ versus *Pkhd1* basolateral medium. Abbreviations: ap, apical medium; bl, basolateral medium.

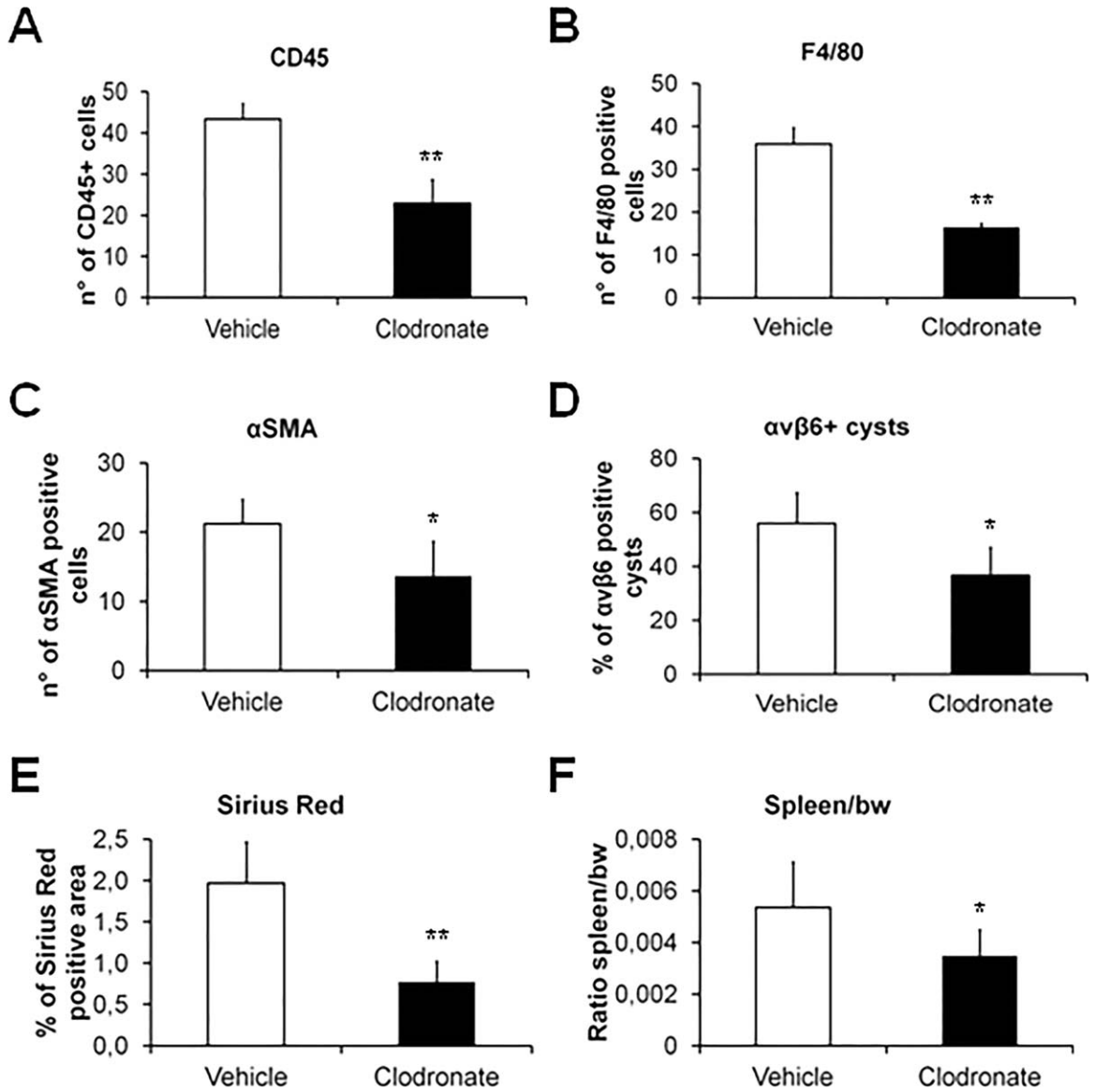

FIG. 7. Macrophage depletion induced by clodronate halts fibrosis progression and development of portal hypertension and reduces αvβ6 integrin biliary expression, macrophage infiltration, and myofibroblast activation in *Pkhd1*$^{del4/del4}$ mice. (A-F) Clodronate treatment resulted in a significant reduction in the number of CD45^{+} (inflammatory cells, A), F4/80^{+} (macrophages, B), and α-SMA^{+} (myofibroblasts, C) cells as well as in the expression of αvβ6 on biliary structures (D) and in portal fibrosis (sirius red staining of the peribiliary area, E). Noteworthy, hampering peribiliary fibrosis at this stage is clinically relevant as it prevents development of portal hypertension, as shown by the significant reduction in splenomegaly (spleen/body weight, F) (n = 3 vehicle, n = 4 clodronate-treated). Representative images of both experimental groups are given in Supporting Fig. S8. *$P < 0.05$ versus vehicle, **$P < 0.01$ versus vehicle. Abbreviation: bw, body weight.

reducing the macrophage transwell migration, reaching an extent comparable to that measured after administration of the β-catenin inhibitors, without any effect on cell viability (Fig. 6A). In *Pkhd1*$^{del4/del4}$ cholangiocytes exposed to β-catenin inhibitors (quercetin or ICG-001), gene expression and protein secretion of CXCL1, CXCL10, and CXCL12 were significantly inhibited (Fig. 6B-D). This finding establishes a mechanistic relationship between the increased production of CXCL1, CXCL10, and CXCL12 and a known signaling defect of *Pkhd1*$^{del4/del4}$ cholangiocytes.

GENE EXPRESSION OF COL1(A1) AND SNAIL1 IS INCREASED IN *PKHD1*$^{DEL4/DEL4}$ CELLS AND FURTHER STIMULATED BY TGFβ1

Because the biological activity of TGFβ1 is enhanced in the vicinity of cells displaying $\alpha v\beta 6$ integrin, we studied the effects of TGFβ1 on COL1(A1) mRNA expression in cultured cholangiocytes, a cell type which is not commonly considered a source of procollagen-I. Compared to WT, *Pkhd1*$^{del4/del4}$ cholangiocytes showed increased basal levels of COL1(A1) mRNA ($P < 0.01$), which were further up-regulated by TGFβ1 (1 ng/mL) ($P < 0.05$). This was not observed in WT cholangiocytes (Supporting Fig. S7A). Similarly, Snail1 mRNA basal levels were higher in *Pkhd1*$^{del4/del4}$ cholangiocytes and were further stimulated by TGFβ1 (Supporting Fig. S7B). Again, increased gene expression of COL1(A1) was confirmed in biliary cysts analyzed after isolation by LCM at 1 month and 3 months (Supporting Fig. S7C). These data are consistent with the observation that TGFβ1 signaling is functionally active in FPC-defective cholangiocytes (Supporting Fig. S5) and that collagen-I, stimulated by locally activated TGFβ1, starts to be deposited in close vicinity to biliary cysts, when myofibroblasts are scarce or absent (Supporting Fig. S7D).

MACROPHAGE DEPLETION BY CLODRONATE IN *PKHD1*$^{DEL4/DEL4}$ MICE TREATED FROM 3 MONTHS TO 6 MONTHS HALTS FIBROSIS PROGRESSION AND DEVELOPMENT OF PORTAL HYPERTENSION AND REDUCES $\alpha V\beta 6$ INTEGRIN BILIARY EXPRESSION, MACROPHAGE INFILTRATION, MYOFIBROBLAST ACTIVATION, AND BILIARY CYST AREA

To confirm the pathogenetic role of macrophages in regulating biliary fibrogenesis in FPC deficiency, we tested the effects of macrophage depletion following a 3-month treatment with clodronate (Supporting Fig. S8A,B). We chose the interval from 3 months through 6 months as the critical window of fibrogenesis preceding the development of portal hypertension. At the end of treatment, the number of macrophages infiltrating the portal space was comparable to that of the starting time, being reduced by about 60% with respect to paired controls (Fig. 7A,B; Supporting Fig. S9A), without significant changes in the proportion between M1 and M2. Interestingly, macrophage depletion was associated with a significant decrease in the expression levels of $\alpha v\beta 6$ on biliary structures (Fig. 7D; Supporting Fig. S9C) and in myofibroblast accumulation in the portal space (Fig. 7C; Supporting Fig. S9B). These effects were accompanied by a striking reduction in sirius red staining of the peribiliary area (Fig. 7E; Supporting Fig. S9D) together with a significant decrease in biliary cysts (Supporting Fig. S8C-E). Noteworthy, reducing peribiliary fibrosis at this stage is clinically relevant as it prevents development of portal hypertension, as shown by the absence of significant splenomegaly in treated mice (Fig. 7F).

Discussion

Portal fibrosis is the main mechanism of chronic liver disease progression. Most experimental studies on liver fibrosis use models of obstructive cholestasis or toxin-induced necroinflammatory biliary or parenchymal damage. However, genetic diseases offer unique opportunities to probe fundamental disease mechanisms. In this study, we investigated the mechanisms of liver fibrosis in CHF, a genetic fibropolycystic liver disorder, characterized by progressive peribiliary fibrosis and portal hypertension.

We show that in CHF fibrosis develops in two phases. During the slowly progressing preclinical phase, bone marrow-derived macrophages are recruited by chemokines secreted by the FPC-defective cystic epithelium. TNFα, secreted by classically activated M1 macrophages, up-regulates epithelial expression of $\alpha v\beta 6$ integrin (an effect specific of FPC-defective cholangiocytes), which then activates latent TGFβ1 in the vicinity of the cystic epithelium. We also found that cholangiocytes respond to TGFβ by producing COL1(A1). While this may actually promote peribiliary fibrosis during the early phases of the disease, further studies are needed to unequivocally demonstrate the ability of these cells to produce collagen. In the early phase infiltrating myofibroblasts are scarce, but their number, essentially represented by portal fibroblasts, increases during the second phase of accelerating fibrogenesis as the proportion of alternatively activated M2 macrophages increases along with the

expression of TGFβ1 and collagen-I and portal hypertension becomes clinically evident. Thus, in CHF a genetically determined dysfunction of epithelial cell homeostasis promotes the secretion of chemokines able to recruit macrophages that orchestrate a profibrotic tissue response switching from an inflammatory to a reparative phenotype.

For these studies, we used an animal model (*Pkhd1*$^{del4/del4}$ mouse) that reproduces the clinical and histological features of human CHF. This model presents unique features compared to other experimental models of portal fibrosis, such as bile duct ligation, sclerosing cholangitis caused by multidrug resistance-2 deficiency,[14,16] or toxicants. In fact, in *Pkhd1*$^{del4/del4}$ mice, fibrosis is not related to a necroinflammatory or obstructive process and the evolution of biliary fibrosis is slow: it resembles that of human CHF, in which portal hypertension occurs in the absence of cirrhosis and is generally diagnosed only late in youth.[17]

In contrast with multidrug resistance-2 knockout mice[13] and bile duct ligation, in which there is an early and massive increase in periportal α-SMA$^+$ myofibroblasts, in *Pkhd1*$^{del4/del4}$ mice, in spite of increased COL1(A1) levels, a significant increase in α-SMA$^+$ cells, mainly related to ELN$^+$ portal myofibroblast[18,19] accumulation, is detected only later, once portal fibrosis is already established. Our data show an early and progressive accumulation of mononuclear CD45$^+$ inflammatory infiltrate in the portal space (mostly macrophages), suggesting that the defect in epithelial cell FPC expression causes a chronic, low-grade inflammatory process and initial collagen deposition. Our findings also indicate that recruited macrophages are likely of bone marrow origin (based on their expression of MAC387),[20] while the contribution of endogenous, yolk sac-derived macrophages (CD68$^+$) is negligible.[21] Studies in archival human CHF specimens confirmed an early portal infiltration with CD45$^+$ cells in the absence of α-SMA$^+$ and ELN$^+$ cells in early cases without portal hypertension, thus indicating that our findings have translational relevance.

This low-grade chronic inflammation (defined by Medzhitov as "parainflammation") is a process of adaptation to an unresolving cell dysfunction or noxious condition.[7] When the cell dysfunction is persistent, the inflammatory response, unable to restore the normal tissue homeostasis, becomes pathologic and stimulates the deposition of scar tissue.[22] Consistent with prior reports showing increased cytokine and growth factor production in fibropolycystic liver diseases,[8,9] our study demonstrates that FPC-defective cholangiocytes produce several chemokines. *In vivo* analysis of transcripts expressed in biliary cysts isolated by LCM from 1-month-old and 3-month-old *Pkhd1*$^{del4/del4}$ shows that expression of specific chemokines (SDF-1/CXCL12, LIX/CXCL5, keratinocyte chemoattractant/CXCL1, IP-10/CXCL10, MIP-2/CXCL2, IL-1β) is increased from the early stages of the disease. Furthermore, we found that the medium of polarized *Pkhd1*$^{del4/del4}$ cholangiocytes is able to recruit macrophages much more intensely than medium from WT cholangiocytes. The recruiting effect of the basolateral medium was much stronger than that of the apical medium, indicating that chemokine secretion is polarized. Measuring the basolateral concentration of a panel of cytokines/chemokines, we confirmed that *Pkhd1*$^{del4/del4}$ cholangiocytes produce increased levels of soluble factors able to recruit macrophages, including MCP-1, CXCL1, CXCL5, CXCL10, and CXCL12. Among the above chemokines, the role of MCP-1 in biliary pathophysiology has been extensively studied; cholangiocytes can secrete MCP-1 in culture[23] and *in vivo*, and following liver damage induced by bile duct ligation or hydrophobic bile acid intoxication, MCP-1 secretion increases together with the extent of portal inflammatory infiltrate.[24,25]

Several signaling defects have been described in FPC-defective cells, including increased cyclic adenosine monophosphate/protein kinase A-mediated Ser^{675}-phosphorylation of β-catenin, leading to enhanced β-catenin transcriptional activity.[5] Recent findings indicate that β-catenin can act as a regulator of inflammation.[5] Consistent with this hypothesis, our data show that in *Pkhd1*$^{del4/del4}$ cholangiocytes gene expression and secretion of CXCL1, CXCL10, and CXCL12 were inhibited by two different inhibitors of β-catenin transcriptional activity (quercetin and ICG-001),[5] suggesting that in FPC deficiency activation of β-catenin signaling promotes a persistent proinflammatory response that recruits macrophages near the biliary cysts. Notably, exposure to basolateral medium from β-catenin-inhibited *Pkhd1*$^{del4/del4}$ cholangiocytes was able to suppress macrophage recruitment to an extent similar to that obtained with the simultaneous antagonism of CXCL1, CXCL10, and CXCL12.

Whole-liver expression of TNFα and TGFβ1 increased significantly in *Pkhd1*$^{del4/del4}$ mice, and their expression in macrophages was stimulated by CXCL1 and CXCL10. Noteworthy, both TNFα and TGFβ1 increased $\alpha v\beta 6$ integrin expression on cholangiocytes,

but inducing effects by TNFα were observed only in *Pkhd1*$^{del4/del4}$ cholangiocytes and were independent from TGFβ1 activation. Expression of αvβ6 integrin was typically restricted to the cystic epithelium, where it was progressively up-regulated over time and strongly correlated with portal fibrosis. Furthermore, αvβ6 expression was accompanied by signatures of TGFβ1 activation in cholangiocytes (Snail1 and pSmad3 nuclear expression), also in human CHF specimens. TGFβ1 is in fact produced as an inactive latent precursor that is locally activated by αvβ6 integrin that cleaves the latency associated peptide.[26]

TNFα and TGFβ1 are expressed by macrophages with proinflammatory (M1) and profibrotic (M2) functions, respectively.[27] During the natural course of a wound-healing response, classically activated macrophages recruited to the site of damage first show a proinflammatory phenotype, with abundant secretion of TNFα. Then, to counteract the tissue-damaging potential of the inflammatory response, macrophages switch to an anti-inflammatory phenotype. If tissue damage persists, macrophages turn into a profibrotic phenotype, whereby TGFβ1 expression is prevalent.[28] Our model is paradigmatic of this sequence, with an initial higher M1 proportion and a progressively increasing M2 contribution, matching that of M1 by 9 months, consistent with the observed time-dependent changes in TNFα and TGFβ1 expression. Interestingly, in addition to CXCL1 and CXCL10, CXCL5, which we found increased early in *Pkhd1*$^{del4/del4}$ biliary cysts *in vivo* by LCM, is also able to stimulate TNFα production in macrophages.[29] Given its early marked increase and its specific effects on epithelial αvβ6 expression on FPC-defective cholangiocytes, TNFα may contribute to local fibrogenesis in *Pkhd1*$^{del4/del4}$ mice, during the early phases of fibrosis, when most TGFβ1 signaling is likely to derive from the activation of latent TGFβ1. Following activation by αvβ6, which occurs at the epithelial cell surface, TGFβ1 exerts its effects within the limits of the site of activation. The ability of reactive cholangiocytes to release fibrogenic growth factors, including platelet-derived growth factor-B,[28] connective tissue growth factor,[30] and extracellular matrix components, such as procollagen-IV[31] and laminin,[32] is well known.[26,27,30] Our data show that in *Pkhd1*$^{del4/del4}$ cholangiocytes procollagen-I transcripts are increased with respect to WT cholangiocytes both *in vitro* and *in vivo* and are remarkably up-regulated by TGFβ1. *In vitro* susceptibility of *Pkhd1*$^{del4/del4}$ cholangiocytes to TGFβ1 effects was confirmed by the concomitant increased gene expression of the TGFβ1-dependent transcription

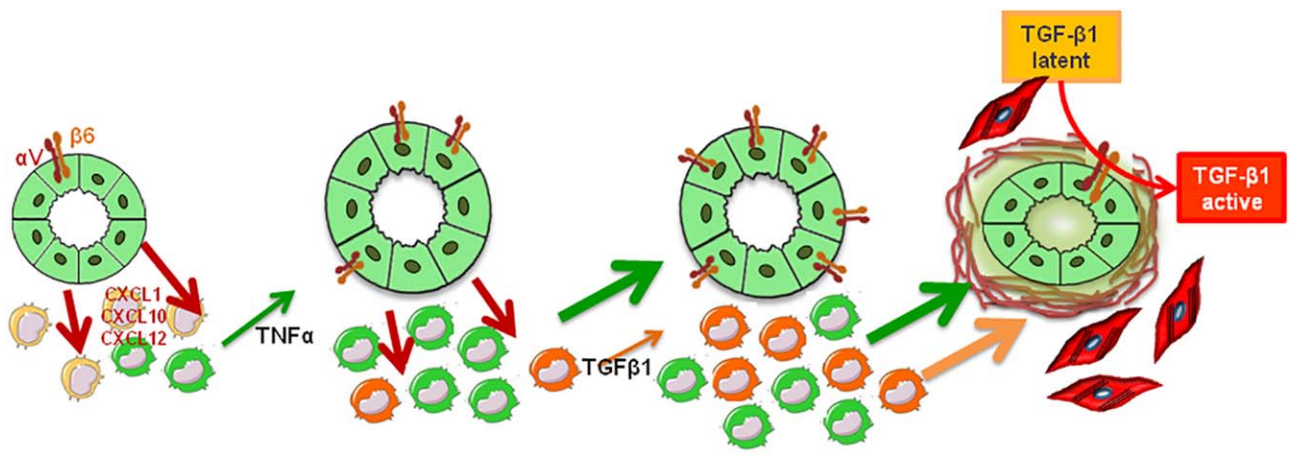

FIG. 8. Working model. Crosstalk between cholangiocytes and macrophages stimulates peribiliary fibrosis in *Pkhd1*$^{del4/del4}$ mice. In *Pkhd1*$^{del4/del4}$ mice, portal fibrosis is the result of intensive crosstalk between epithelial and inflammatory cells, originating from FPC-deficient cholangiocytes. By secreting a range of chemokines, including CXCL1, CXCL10, and CXCL12, likely secondary to β-catenin signaling overactivation, *Pkhd1*$^{del4/del4}$ cholangiocytes recruit macrophages in the portal area and stimulate their secretory functions. In the early phases, this portal infiltrate is mainly composed of M1 macrophages (green peribiliary cells), and TNFα (green arrow) is the predominant cytokine released until also TGFβ1 (orange arrow) becomes significantly secreted by M2 macrophages (orange peribiliary cells). Both macrophage-derived cytokines up-regulate αvβ6 integrin expression on biliary cysts and this, in turn, activates latent TGFβ1. Once activated, TGFβ1 induces production of collagen by cyst cholangiocytes and, as the disease progresses, by myofibroblasts, ultimately resulting in excessive matrix deposition into the peribiliary region.

factor Snail1. The concentration of TGFβ1 used for *in vitro* experiments (1 ng/mL) is in the range of this cytokine found with tissue analysis. Higher TGFβ1 concentrations have an apoptotic effect on cholangiocytes in culture. Interestingly, in the same experimental model, we have recently shown that *Pkhd1*$^{del4/del4}$ cholangiocytes possess increased β-catenin-dependent migratory properties.[5] Increased migration and abnormal collagen deposition are consistent with the concept that FPC-defective epithelial cells are more prone to perform some limited mesenchymal functions. The direct involvement of cholangiocytes in driving collagen deposition, at least in the initial phase of fibrogenesis in *Pkhd1*$^{del4/del4}$ mice, may explain the distinctive features of this model, including the early peribiliary and slowly evolving matrix deposition. However, mesenchymal properties acquired by epithelial cells *in vitro* should be interpreted with caution, and further studies *in vivo* using mice reporter lines may help to clarify the question. After 6 months, when fibrosis accelerates and clinically relevant portal hypertension begins, ELN^{+} portal myofibroblasts become the relevant source of collagen.

The *in vivo* experiments with clodronate in *Pkhd1*$^{del4/del4}$ mice are consistent with this working model. By targeting macrophage infiltration at an age when portal hypertension is not yet developed, we were able to show a stark reduction in macrophage infiltration and decreases in $\alpha v\beta 6$ biliary expression and in portal myofibroblast accumulation. These phenotypic alterations related to macrophage depletion are pathophysiologically relevant as they block progression of biliary fibrosis and prevent the development of portal hypertension. As a consequence of the reduction in macrophage infiltration, a reduction in the liver cyst area was noted, supporting the concept that macrophages exert a stimulatory effect on cyst growth.

In conclusion, we have shown that development of fibrosis in CHF follows a novel paradigm based on a complex interplay between epithelial, innate inflammatory, and mesenchymal cells (Fig. 8). These mechanisms suggest new, disease-specific targets for antifibrotic therapies in CHF, a topic worth addressing in future studies.

Acknowledgment: We thank Sheila Violette (Stromedix Inc.) for kindly providing the TGFβRII blocking antibody, Stephan Somlo (Yale University) for the gift of *Pkhd1*$^{del4/del4}$ mice, and Rafaz Hoque (Yale University) for help with fluorescence-activated cell sorting analysis. Alberto Mantovani (University of Milan), Ruslan Medzhitov (Yale University), and Maurizio Parola (University of Turin) are gratefully acknowledged for critical revision of the manuscript and helpful comments. We are indebted to Michele Colledan and Aurelio Sonzogni (Papa Giovanni XXIII Hospital) and to Paola Francalanci (Bambino Gesù Pediatric Hospital) for providing histological samples of CHF patients, as well as to Davide Viganò (University of Sassari) for help with Boyden chamber experiments.

REFERENCES

1) Ward CJ, Yuan D, Masyuk TV, Wang X, Punyashthiti R, Whelan S, et al. Cellular and subcellular localization of the ARPKD protein; fibrocystin is expressed on primary cilia. Hum Mol Genet 2003;12:2703-2710.
2) **Zhang MZ, Mai W, Li C**, *Cho SY, Hao C, Moeckel G, et al. PKHD1 protein encoded by the gene for autosomal recessive polycystic kidney disease associates with basal bodies and primary cilia in renal epithelial cells*. Proc Natl Acad Sci USA 2004;101:2311-2316.
3) Lazaridis KN, Strazzabosco M, Larusso NF. The cholangiopathies: disorders of biliary epithelia. Gastroenterology 2004;127: 1565-1577.
4) Nakanuma Y, Harada K, Sato Y, Ikeda H. Recent progress in the etiopathogenesis of pediatric biliary disease, particularly Caroli's disease with congenital hepatic fibrosis and biliary atresia. Histol Histopathol 2010;25:223-235.
5) Spirli C, Locatelli L, Morell CM, Fiorotto R, Morton SD, Cadamuro M, et al. PKA dependent p-Ser^{675} β-catenin, a novel signaling defect in a mouse model of congenital hepatic fibrosis. HEPATOLOGY 2013;58:1713-1723.
6) Anson M, Crain-Denoyelle AM, Baud V, Chereau F, Gougelet A, Terris B, et al. Oncogenic beta-catenin triggers an inflammatory response that determines the aggressiveness of hepatocellular carcinoma in mice. J Clin Invest 2012;122:586-599.
7) Medzhitov R. Origin and physiological roles of inflammation. Nature 2008;454:428-435.
8) Nichols MT, Gidey E, Matzakos T, Dahl R, Stiegmann G, Shah RJ, et al. Secretion of cytokines and growth factors into autosomal dominant polycystic kidney disease liver cyst fluid. HEPATOLOGY 2004;40:836-846.
9) Fabris L, Cadamuro M, Fiorotto R, Roskams T, Spirlì C, Melero S, et al. Effects of angiogenic factor overexpression by human and rodent cholangiocytes in polycystic liver diseases. HEPATOLOGY 2006;43:1001-1012.
10) Gallagher AR, Esquivel EL, Briere TS, Tian X, Mitobe M, Menezes LF, et al. Biliary and pancreatic dysgenesis in mice harboring a mutation in *Pkhd1*. Am J Pathol 2008;172:417-429.
11) de Meijer VE, Sverdlov DY, Popov Y, Le HD, Meisel JA, Nosé V, et al. Broad-spectrum matrix metalloproteinase inhibition curbs inflammation and liver injury but aggravates experimental liver fibrosis in mice. PLoS One 2010;5:e11256.
12) Sato A, Nakashima H, Nakashima M, Ikarashi M, Nishiyama K, Kinoshita M, et al. Involvement of the TNF and FasL produced by CD11b Kupffer cells/macrophages in CCl4-induced acute hepatic injury. PLoS One 2014;9:e92515.
13) **Popov Y, Patsenker E**, *Fickert P, Trauner M, Schuppan D. Mdr2 (*Abcb4*)$^{-/-}$ mice spontaneously develop severe biliary fibrosis via massive dysregulation of pro- and antifibrogenic genes. J Hepatol 2005;43:1045-1054.*

14) Popov Y, Patsenker E, Stickel F, Zaks J, Bhaskar KR, Niedobitek G, et al. Integrin αVβ6 is a marker of the progression of biliary and portal liver fibrosis and a novel target for antifibrotic therapies. J Hepatol 2008;48:453-464.
15) Teicher BA, Fricker SP. CXCL12 (SDF-1)/CXCR4 pathway in cancer. Clin Cancer Res 2010;16:2927-2931.
16) Patsenker E, Popov Y, Stickel F, Jonczyk A, Goodman SL, Schuppan D. Inhibition of integrin αVβ6 on cholangiocytes blocks TGF-β activation and retards biliary fibrosis progression. Gastroenterology 2008;135:660-670.
17) O'Brien K, Font-Montgomery E, Lukose L, Bryant J, Piwnica-Worms K, Edwards H, et al. Congenital hepatic fibrosis and portal hypertension in autosomal dominant polycystic kidney disease. J Pediatr Gastroenterol Nutr 2012;54:83-89.
18) Dranoff JA, Wells RG. Portal fibroblasts: underappreciated mediators of biliary fibrosis. Hepatology 2010;51:1438-1444.
19) Fausther M, Lavoie EG, Dranoff JA. Contribution of myofibroblasts of different origins to liver fibrosis. Curr Pathobiol Rep 2013;1:225-230.
20) Antoniades CG, Quaglia A, Taams LS, Mitry RR, Hussain M, Abeles R, et al. Source and characterization of hepatic macrophages in acetaminophen-induced acute liver failure in humans. Hepatology 2012;56:735-746.
21) Sica A, Invernizzi P, Mantovani A. Macrophage plasticity and polarization in liver homeostasis and pathology. Hepatology 2014;59:2034-2042.
22) Sica A, Mantovani A. Macrophage plasticity and polarization: *in vivo* veritas. J Clin Invest 2012;122:787-795.
23) Morland CM, Fear J, McNab G, Joplin R, Adams DH. Promotion of leukocyte transendothelial cell migration by chemokines derived from human biliary epithelial cells in vitro. Proc Assoc Am Physicians 1997;109:372-382.
24) Hsieh CS, Huang CC, Wu JJ, Chaung HC, Wu CL, Chang NK, et al. Ascending cholangitis provokes IL-8 and MCP-1 expression and promotes inflammatory cell infiltration in the cholestatic rat liver. J Pediatr Surg 2001;36:1623-1628.
25) Lamireau T, Zoltowska M, Levy E, Yousef I, Rosenbaum J, Tuchweber B, et al. Effects of bile acids on biliary epithelial cells: proliferation, cytotoxicity, and cytokine secretion. Life Sci 2003; 72:1401-1411.
26) Munger JS, Huang X, Kawakatsu H, Griffiths MJ, Dalton SL, Wu J, et al. The integrin αVβ6 binds and activates latent TGF-β1: a mechanism for regulating pulmonary inflammation and fibrosis. Cell 1999;96:319-328.
27) Duffield JS, Forbes SJ, Constandinou CM, Clay S, Partolina M, Vuthoori S, et al. Selective depletion of macrophages reveals distinct, opposing roles during liver injury and repair. J Clin Invest 2005;115:56-65.
28) Wynn TA, Chawla A, Pollard JW. Macrophage biology in development, homeostasis and disease. Nature 2013;496:445-455.
29) Vieira SM, Lemos HP, Grespan R, Napimoga MH, Dal-Secco D, Freitas A, et al. A crucial role for TNF-alpha in mediating neutrophil influx induced by endogenously generated or exogenous chemokines, KC/CXCL1 and LIX/CXCL5. Br J Pharmacol 2009;158:779-789.
30) Fabris L, Strazzabosco M. Epithelial-mesenchymal interactions in biliary diseases. Semin Liver Dis 2011;31:11-32.
31) Milani S, Herbst H, Schuppan D, Hahn EG, Stein H. *In situ* hybridization for procollagen types I, III and IV mRNA in normal and fibrotic rat liver: evidence for predominant expression in nonparenchymal liver cells. Hepatology 1989;10:84-92.
32) Milani S, Herbst H, Schuppan D, Riecken EO, Stein H. Cellular localization of laminin gene transcripts in normal and fibrotic human liver. Am J Pathol 1989;134:1175-1182.

Author names in bold denote shared co-first authorship.

Supporting Information

Additional Supporting Information may be found at onlinelibrary.wiley.com/doi/10.1002/hep.28382/suppinfo.